

Re: “Interactive comment on ‘Effects of vegetation structure on biomass accumulation in a Balanced Optimality Structure Vegetation Model (BOSVM v1.0)’, Anonymous Referee #1”

Z. Yin, S. C. Dekker, B. J. J. M. van den Hurk, H. A. Dijkstra

1. “This is a very interesting paper about the theoretical physical description of the impact of canopy patchiness on biomass production along aridity gradients. A new model able to represent key feedback mechanisms is presented. The F90 source code is provided as a supplement material. The model capitalizes on the LPJ dynamic vegetation model and on pre-existing land surface models (ISBA-A-gs and TESSEL).”

A: Thanks for your positive comments on our work.

2. “For example, the limitations of the approach are not sufficiently described.”

A: A paragraph will be added to discuss the limitation of this research at the end of the discussion section, as “As our interest is to study the effects of vegetation structure on their total biomass between different climate regime, we realize that numerous factors that can significantly influence biomass dynamics are not taken into account. For instance, Dardel et al. [2014] found that the heterogeneities in soil types is an important driver of vegetation-climate interactions. The property of the soil determines soil water holding capacity, which in turn affects the soil water balance. Also we did not include grass-tree competition. Due to this competition, maximum biomass of grasses and woody plants can be limited. Further grasses prohibit the colonization rate of seedlings [Baudena et al., 2010] as they compete for the same resources and grasses provide fuel for fire occurrence [Staver et al., 2011] in savanna systems, which further limit the biomass of woody plants. Moreover, human activities [Kleidon, 2006] and topography [Klausmeier, 1999] have potential effects on dynamics of the ecosystem under certain climate regime, which are not considered in this work. Understanding the importance of climate regimes versus different heterogeneity of local conditions and other important mechanisms in savanna ecosystems soil types to simulate biomass dynamics will be a interesting and important new step.”

3. “In the present version of the text, it is difficult to understand whether or not soil hydrology (2 layers) is consistent with a detailed root profile.”

A: In BOSVM, we didn’t include detailed root profile. We only consider the effects of total amount of root biomass (C_{root}) per canopy area (CA) on soil water stress. We will

clarify this in the new version.

4. “It is difficult to understand whether or not radiative transfer within vegetation is consistent with patchiness (impact of clumping on light absorption ?).”

A: Here we assume a spherical leaf angle distribution. Thus, the radiative transfer within vegetation is only influenced by leaf area index (see Appendix B4) and not with clumping effects. We have chosen for this, to keep the model balanced, i.e. that the complexity of climate, physiology, ecology and hydrology mechanisms are balanced within our model. We will clarify in the manuscript that leaf angles are randomly distributed and that we do not account for clumping.

5. “Although the new model represents many feedbacks, other (biological / soil) feedbacks may be at stake in the real world. For example, what about competition between grass and trees ? Impact of the soil water holding capacity ?”

A: The vegetation dynamics is influenced by numerous internal/external variables and complex interactions among them. Detailed ecological models of savanna systems are developed (e.g. Scheiter and Higgins [2009]), but these models are too complex to couple to global climate models to understand climate-vegetation feedbacks. Alternatively, the current dynamic vegetation models used in earth system models do not account for important ecological mechanisms as small scale vegetation structure, different vegetation types and different plant specific defensive/offensive water use mechanisms with different impacts on fire and e.g. heterogeneities of microtopography and soil properties. As mentioned under point 2, we will add a paragraph in the discussion on the limitation and other potential impacts and mechanisms such as tree-grass competition.

6. “PP. 4603-4604: Title sounds different from the contents of the abstract. Is the objective of the paper to present a new model or to propose an interpretation of the vegetation patchiness in semiarid regions ? ”BOSVM” is used in the title only. For the sake of clarity, title should be modified.”

A: The primary objective is to investigate the effect of vegetation structure on its total biomass and find the optimal structure that can lead to the maximum total biomass under given climate. To address this question, the new water-carbon-energy balanced model is developed. Most important reason for developing this model is that it can be linked to an atmospheric model for further land-atmosphere interactions research. The name of the model was added temporarily as a requirement before publication on GMDD. The model’s name and the rationale for the development of the model will be updated in the introduction of the manuscript.

7. “P. 4606, L. 16: the work of Dardel et al., Re-greening Sahel: 30 years of remote sensing data and field observations (Mali, Niger), Remote Sens. Environ., 2014, could be cited as it shows that soil type is a key driver of the vegetation response to climate in Sahel.”

A: Will be cited. Also we will add in the introduction: “Although soil types do play an

important role in vegetation response to climate [Dardel et al., 2014], its distribution is independent to the precipitation gradient. Thus, we only applied medium soil texture [Balsamo et al., 2009] in this study and ignore effects of soil types on biomass dynamics.”

8. “P. 4610 (Sect. 2.2): It is not clear how plant growth is related to photosynthesis.”

A: In Section 2.2, we will add: “During the photosynthesis simulation, we calculate NPP (see Appendix B). Then based on Eq 3, the total biomass is updated, after which vegetation structural variables are updated by equations listed in Section 2.2. First, C_{root} and $C_{\text{leaf}} + C_{\text{stem}}$ can be calculated by α (Eq 5). Second, $C_{\text{leaf}} + C_{\text{stem}}$ can be represented as a function of LAI and CA by combining Eq 6 and 7. Then, LAI and CA can be retrieved by the combined equation and Equation 8. Third, CA is compared to CA_{ref} . If $CA > CA_{\text{ref}}$, LAI will be recalculated by the combined equation while keeping $CA = CA_{\text{ref}}$ (CA cannot exceed CA_{ref}). At last, f_c and φ can be obtained by Eq 9 and 10 respectively.”

In the Section 2.8, we will add: “... After updating the C_{veg} , other structural variables can be updated as described above.”

9. “P. 4611 (Table 1): please check the Dmax units in Table 1.”

A: Corrected (see Table 1 below).

10. “P. 4611 (Eq. 9): The vegetation cover fraction changes with time. Is the (carbon) mass conservation ensured ? How ? Same question for soil water mass conservation.”

A: Yes. The carbon mass conservation is governed by Eq 3. At the end of each time step, the total biomass is updated by Eq 3. Then the vegetation structural variables are updated (see the reply to comment 8). The soil water mass conservation is governed by Eq 2.

11. “P. 4612, L. 21 (Table 1): the gamma value for grass indicates that C3 grasses are considered, not C4 grasses. In west Africa, are C3 grasses frequent ? I would expect C4 grass species are more frequent than C3 grass species.”

A: True. C4 grasses are more common than C3 grasses in Africa. We revised the parameterization and simulation of grasses. Parameterization in Table 1 is updated (see below). Figure 2, 7, 8, 9 and 10 are updated (see below). In Figure 7, we can find that areas of survival patterns of C4 grasses are larger than C3 grasses (Figure 7 in previous version), which coincides with that C4 species is more common than C3 species in arid and semi-arid areas. However, the new parameterization of C4 grasses has no different effect on model behavior.

12. “P. 4617, L. 11: ”stomatal opening until very dry”; I suppose that this depends on the parameters of the model and how the drought-tolerant parameterization is implemented ?”

A: True. The threshold (f_{wc} in Table 1) here is determined by the parameterization

based on observations [Calvet, 2000, Calvet et al., 2004]. Also, it depends on soil types and root density (see Eq 12). Although the soil type is fixed (medium) in our research, the biomass dynamics can change the threshold significantly (by Eq 12). We will change this accordingly.

13. “P. 4620, L. 19: It would be useful here to detail the time steps of the various processes (e.g. hourly for photosynthesis ? Daily for biomass ?)”

A: In this work, we use half an hour time step in the simulation for all processes. It is modified as: “... modifies the soil temperature (Appendix C2). The time step (dt) of the simulation is half an hour for all processes.”

14. “P. 4620, L. 21: This is the first and the last time we see a map of west Africa. This is confusing. Were continuous model simulations performed over this area ? If yes, what do the simulated variables (e.g. LAI) look like ? Are they consistent with published satellite or in situ observations ?”

A: No. We didn’t apply the model for the whole area shown in the map, as our interest is the sensitivity of total biomass to vegetation structure. The spatial implementation is provided in the next paper including fire behaviour (in Earth System Dynamics Discussion now, doi:10.5194/esdd-5-83-2014). A paragraph will be added in Section 2.9 as: “Since this study focuses on the effect of vegetation structure on total biomass across the precipitation gradient, the BOSVM model is not applied to the whole region of West Africa. In the second experiment (Section 3.2), four grid cells with mean annual precipitation of 200 mm yr^{-1} , 400 mm yr^{-1} , 800 mm yr^{-1} and 1200 mm yr^{-1} (black points in Fig 5) are chosen as climate forcing to represent the gradient of rainfall. In the third experiment (Section 3.3), we provide the model simulation for a sub region (the dashed rectangle in Fig 5).” Finally we will add an extra model testing based on observations of woody cover across climate regimes from 100 to 1500 mm yr^{-1} , also requested by Referee #2. Details are given in the reply of Referee #2, resulting in a new figure 11.

The caption of Fig 5 is revised as: “Annual mean precipitation and incoming shortwave radiation distribution in West Africa. The four black points are chosen as climate forcings for the second experiment (Section 3.2). The Rectangle marked is the study domain in the third experiment (Section 3.3), ranging $[20^\circ\text{W}, 30^\circ\text{E}] \times [5^\circ\text{S}, 20^\circ\text{N}]$ in West Africa. Data is from the ALMIP forcing data set [Boone et al., 2009].”

15. “P. 4621, L. 15: using CA/CA_{ref} in Fig. 6 (instead of CA) would be more appropriate.”

A: True. Revised. The caption of Fig 6 is modified as: “Patterns of woody vegetation for different combinations of α and D . α is varied from 0 to 0.5. D is set from 0.1 to 5. Total biomass is 30 kg C per pixel of 15 m^2 . Panel (a): LAI; (b): relative CA ; (c): f_c ; (d): relative φ . Relative CA is defined as CA/CA_{ref} . Relative φ is defined as $\varphi/\varphi_{\text{max}}$. When $\varphi > \varphi_{\text{max}}$, value of relative φ is set to one.”

16. “P. 4622, L. 24: please explain why WUE increases.”

A: The explicit explanation is in Section 2.6 and Figure 2. Here it will be modified as: “... the water use efficiency increases with extractable water (Section 2.6 and Fig 2).”

17. “P. 4626, L. 5: why 87 grid cells ?”

A: 87 grid cells are those grid cells in the research region (dashed rectangle in the Fig. 5) where woody plants are able to exist. It will be revised to: “To depict the variability of the response mechanisms as a function of the climate regime, we calculated Spearman’s correlation coefficients between averaged biomass and variables LAI, f_c and WUE under each given climate regime for each vegetation strategy. For each grid cell in the research region (dashed rectangle in Fig 5) and for each vegetation strategy, we simulated biomass of 100 vegetation structures as defined in Sect. 3.2. Thus we have 100 samples of simulated average biomass, LAI, f_c and WUE, which are used to calculate correlation coefficients.”

18. “P. 4627, L. 24: ”fc-Rspace feedback” should be defined here. Do you refer to Eq. (25) ?”

A: Since we introduce and discuss f_c-R_{WU} and f_c-R_{space} together, we think it’s better to keep the definition of R_{space} in Section 2.7. Here we will mention Eq. 25 when f_c-R_{space} is introduced.

19. “P. 4632 (A2, Table 1): why are the ”defensive / offensive” columns omitted for grass ? The two parameterizations are considered in a number of figures. The corresponding parameters should be indicated in Table 1.”

A: True. Corrected (see below in the new table captions).

20. “Figures 7-9: (a, c) why not exploring values of alpha higher than 0.5 ? (b, d) what is the meaning of the crosses ? Do they correspond to various values of D and alpha ? Please explain”

A: Because if α is larger than 0.5, above ground biomass will be larger than the rooting biomass, which is not normal (see the LPJ model [Sitch et al., 2003]). We will clarify this in the new manuscript.

Yes. Crosses in sub figures (b,d) are averaged value of variables (C_{veg} , LAI, f_c , WUE, etc.) corresponding to 100 vegetation structures.

It will be revised as: “Figure 7b shows relations of C_{veg} -LAI, C_{veg} - f_c , C_{veg} -WUE and f_c - R_{WU} . Each cross corresponds to a specific vegetation structure.”

21. “Figures 6-9: the scale for D is quite strange. It seems that what is plotted is a complex function of D, not D.”

A: Yes. As D is a ratio of relative LAI to relative CA, it can vary from 0 to ∞ . Thus the distribution of D value in Fig 6–9 is determined by an inverse tangent function. It will be revised as: “The scale of D (y-axis) follows an inverse tangent function. Same for Fig. 7–9.”

22. “P. 4608, L. 3: ”Obkhov” ?”

A: Corrected.

23. “P. 4608, L. 19: ”In stead” ?”

A: Corrected.

24. “P. 4610, L. 10: ”exists of” or ”consists of” ?”

A: Corrected.

25. “P. 4610, L. 12 (Fig. 1): please explain Fig. 1 more extensively. This figure could be split into 4 figures.”

A: Figure 1 will be referred in places where it is mentioned.

26. “P. 4610, L. 17 (and Eq. 5): this is not ”shoot-root ratio”, Eq. (5) corresponds to the ”shoot-total biomass ratio”. This is confusing. Either change Eq. (5) or rename alpha.”

A: Renamed α as “shoot-total biomass ratio”.

27. “P. 4611, L. 13 (and Eq. 8): is it ”between relative LAI and relative CA” or ”between relative LAI and relative CA” ? This is confusing. Either change Eq. (8) or rename D.”

A: It is modified as: “The second control parameter, representing the trade-off between CA and LAI, is the ratio of relative CA to relative LAI (Eq. 8).”

28. “P. 4612, L. 2-6: this is difficult to understand as it was not explained in which order the variables are calculated. Refer to Figure 4 here ?”

A: Here we want to explain that the canopy structure of vegetation will change when $CA=CA_{ref}$. When $CA < CA_{ref}$, both CA and LAI increase with the growth of biomass to keep the vegetation structure parameter D as a constant. However, when CA reaches CA_{ref} , vegetation cannot spread laterally anymore. Only LAI can increase with the growth of biomass, suggesting that canopy structure becomes more vertical and D increases (Eq 8). This special case is explicitly explained in the end of Section 2.2. See reply to comment 8.

29. “P. 4617, L. 11: ”remaining” or ”maintaining” ?”

A: Corrected.

30. “P. 4618, L. 15 (Fig. 3): please use colors.”

A: Updated.

31. “P. 4622, L. 21: ”coefficiencies” ?”

A: Corrected.

32. “P. 4623, L. 11: ”different with” ?”

A: Corrected.

33. “P. 4626, L. 23: ”effect” or ”affect” ?”

A: Corrected.

34. “P. 4627, L. 19; ”addtion” ?”

A: Corrected.

Bibliography

G. Balsamo, A. Beljaars, K. Scipal, P. Viterbo, B. van den Hurk, M. Hirschi, and A.K. Betts. A revised hydrology for the ecmwf model: Verification from field site to terrestrial water storage and impact in the integrated forecast system. *Journal of hydrometeorology*, 10(3):623–643, 2009.

M. Baudena, F. D’Andrea, and A. Provenzale. An idealized model for tree–grass coexistence in savannas: the role of life stage structure and fire disturbances. *Journal of Ecology*, 98(1):74–80, 2010.

A. Boone, P. Rosnay, G. Balsamo, A. Beljaars, F. Chopin, B. Decharme, C. Delire, A. Ducharne, S. Gascoin, M. Grippa, F. Guichard, Y. Gusev, P. Harris, L. Jarlan, L. Kergoat, E. Mougin, O. Nasonova, A. Norgaard, T. Orgeval, C. Ottlé, I. Pocard-Leclercq, J. Polcher, I Sandholt, S. Saux-Picart, C. Taylor, and Y. Xue. The AMMA Land Surface Model Intercomparison Project (ALMIP). *Bulletin of the American Meteorological Society*, 90(12):1865–1880, 2013/09/05 2009. doi: 10.1175/2009BAMS2786.1. URL <http://dx.doi.org/10.1175/2009BAMS2786.1>.

J. C. Calvet. Investigating soil and atmospheric plant water stress using physiological and micrometeorological data. *Agricultural and Forest Meteorology*, 103(3):229–247, 2000.

J. C. Calvet, V. Rivalland, C. Picon-Cochard, and J. M. Guehl. Modelling forest transpiration and co₂ fluxes-response to soil moisture stress. *Agricultural and Forest Meteorology*, 124(3):143–156, 2004.

C. Dardel, L. Kergoat, P. Hiernaux, E. Mougin, M. Grippa, and C. J. Tucker. Re-greening sahel: 30 years of remote sensing data and field observations (mali, niger). *Remote Sensing of Environment*, 140(0):350–364, 1 2014. doi: <http://dx.doi.org/10.1016/j.rse.2013.09.011>. URL <http://www.sciencedirect.com/science/article/pii/S0034425713003325>.

C.A. Klausmeier. Regular and irregular patterns in semiarid vegetation. *Science*, 284 (5421):1826–1828, 1999.

- A. Kleidon. The climate sensitivity to human appropriation of vegetation productivity and its thermodynamic characterization. *Global and Planetary Change*, 54(1):109–127, 2006.
- S. Scheiter and S. I. Higgins. Impacts of climate change on the vegetation of africa: an adaptive dynamic vegetation modelling approach. *Global Change Biology*, 15(9):2224–2246, 2009. doi: 10.1111/j.1365-2486.2008.01838.x. URL <http://dx.doi.org/10.1111/j.1365-2486.2008.01838.x>.
- S. Sitch, B. Smith, I. C. Prentice, A. Arneth, A. Bondeau, W. Cramer, J. O. Kaplan, S. Levis, W. Lucht, M. T. Sykes, K. Thonicke, and S. Venevsky. Evaluation of ecosystem dynamics, plant geography and terrestrial carbon cycling in the lpj dynamic global vegetation model. *Global Change Biology*, 9(2):161–185, 2003. doi: 10.1046/j.1365-2486.2003.00569.x. URL <http://dx.doi.org/10.1046/j.1365-2486.2003.00569.x>.
- A. C. Staver, S. Archibald, and S. A. Levin. The global extent and determinants of savanna and forest as alternative biome states. *Science*, 334(6053):230–232, 2011.

Table 1: Parameterization of vegetation with two strategies.

| Parameters | Unit | Vegetation Type | | | | Reference |
|--|-------------------------------------|-----------------|-----------|-----------|-----------|--|
| | | Grass | | Woody | | |
| | | Defensive | Offensive | Defensive | Offensive | |
| $A_{\max}(25\text{ }^{\circ}\text{C})$ | $\text{mg C m}^{-2} \text{ s}^{-1}$ | 0.464 | 0.464 | 0.49 | 0.49 | Boussetta et al. (2013) |
| a_1 | kg C m^{-2} | – | – | 0.65 | 0.65 | Cox (2001) |
| D_{\max} | g kg^{-1} | – | – | 100 | 100 | Calvet et al. (2004) |
| D_{\max}^N | g kg^{-1} | 55 | – | – | – | Calvet (2000) |
| D_{\max}^X | g kg^{-1} | – | 300 | – | – | Calvet (2000) |
| f_0^* | – | – | – | 0.606 | 0.46 | Calvet (2000); Calvet et al. (2004) |
| f_0 | – | 0.6 | 0.6 | – | – | Boussetta et al. (2013) |
| f_{wc} | $\text{m}^2 \text{ m}^{-2}$ | 0.5 | 0.5 | 0.1 | 0.6 | Calvet (2000); Calvet et al. (2004) |
| $g_m^*(25\text{ }^{\circ}\text{C})$ | mm s^{-1} | 2.38 | 2.38 | 1.6 | 4.4 | Calvet (2000); Calvet et al. (2004) |
| $\Gamma(25\text{ }^{\circ}\text{C})$ | ppm | 2.8 | 2.8 | 42 | 42 | Boussetta et al. (2013) |
| ϵ_0^* | $10^{-3} \text{ mg C J}^{-1}$ | 3.82 | 3.82 | 4.64 | 4.64 | Boussetta et al. (2013) |
| $T_{1,\text{Am}}$ | $^{\circ}\text{C}$ | 13 | 13 | 8 | 8 | Calvet (2000) |
| $T_{2,\text{Am}}$ | $^{\circ}\text{C}$ | 38 | 38 | 38 | 38 | Calvet (2000) |
| $T_{1,\text{g}}$ | $^{\circ}\text{C}$ | 13 | 13 | 5 | 5 | Calvet (2000) |
| $T_{2,\text{g}}$ | $^{\circ}\text{C}$ | 36 | 36 | 36 | 36 | Calvet (2000) |
| τ_{leaf} | yr | 1 | 1 | 1 | 1 | – |
| τ_{stem} | yr | – | – | 10 | 10 | – |
| τ_{root} | yr | 1 | 1 | 10 | 10 | – |
| φ_{\max} | kg C m^{-2} | 1 | 1 | 10 | 10 | – |

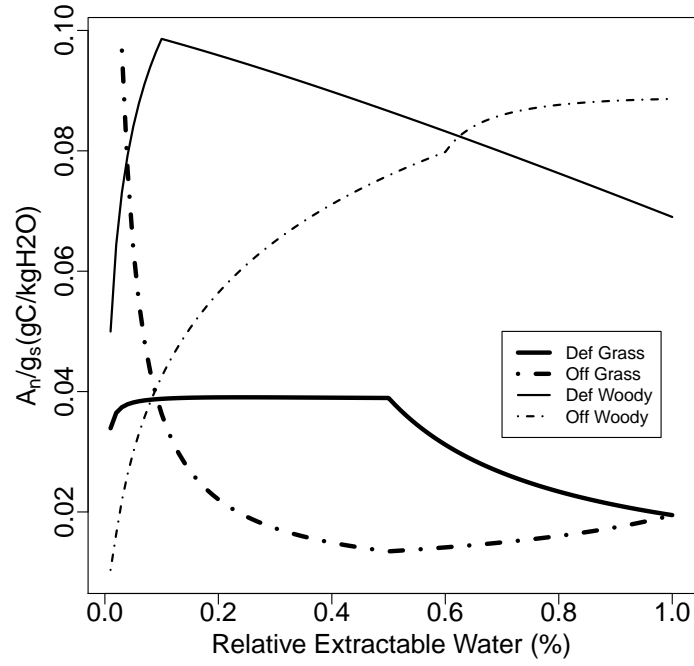


Figure 2: Intrinsic WUE as a function of extractable water. Extractable water (f_w) is defined as Eq. (12). Solid and dot-dashed lines represent defensive and offensive strategies respectively. Thick and thin lines represents grass and woody plants respectively. $vpD = 12 \text{ g kg}^{-1}$, $LAI = 1$, $R_{swd} = 800 \text{ W m}^{-2}$, $c_a = 380 \text{ ppm}$ and $T_s = 25 \text{ }^\circ\text{C}$.

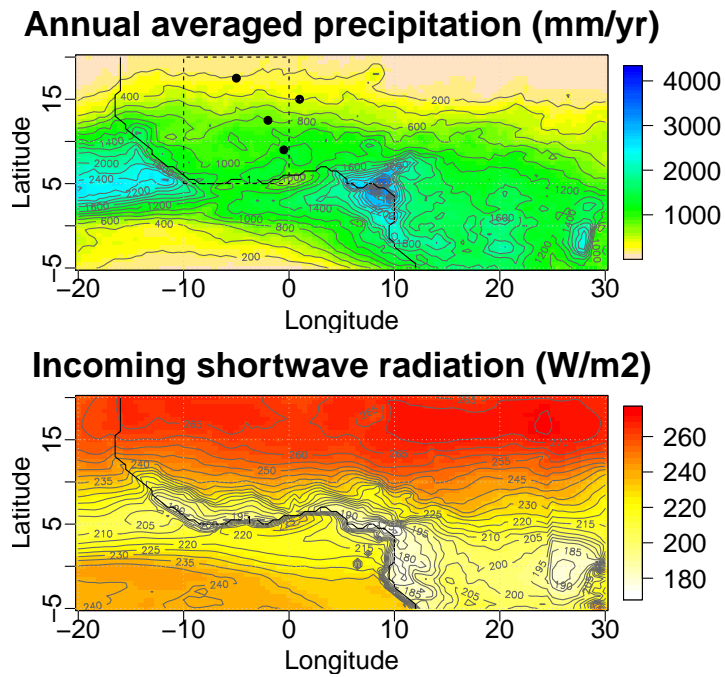


Figure 5: Annual mean precipitation and incoming shortwave radiation distribution in West Africa. The four black points are chosen as climate forcings in the second experiment (Section 3.2). The Rectangle marked is the study domain in the third experiment (Section 3.3), ranging between 20° W to 30° E and from 5° S to 20° N in West Africa. Data is from the ALMIP forcing data set [Boone et al., 2009].

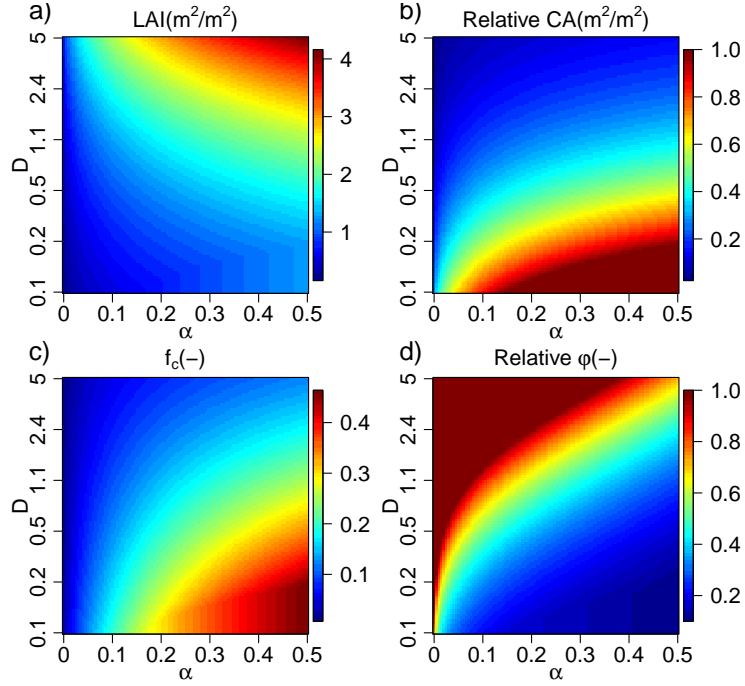


Figure 6: Patterns of woody vegetation for different combinations of α and D . α is varied from 0 to 0.5. D is set from 0.1 to 5. Total biomass is 30 kg C per pixel of 15 m². Panel (a): LAI; (b): relative CA; (c): f_c ; (d): relative φ . Relative CA is defined as CA/CA_{ref} . Relative φ is defined as $\varphi/\varphi_{\text{max}}$. When $\varphi > \varphi_{\text{max}}$, value of relative φ is set to one. The scale of D (y-axis) follows an inverse tangent function. Same for Fig. 7 to 9.

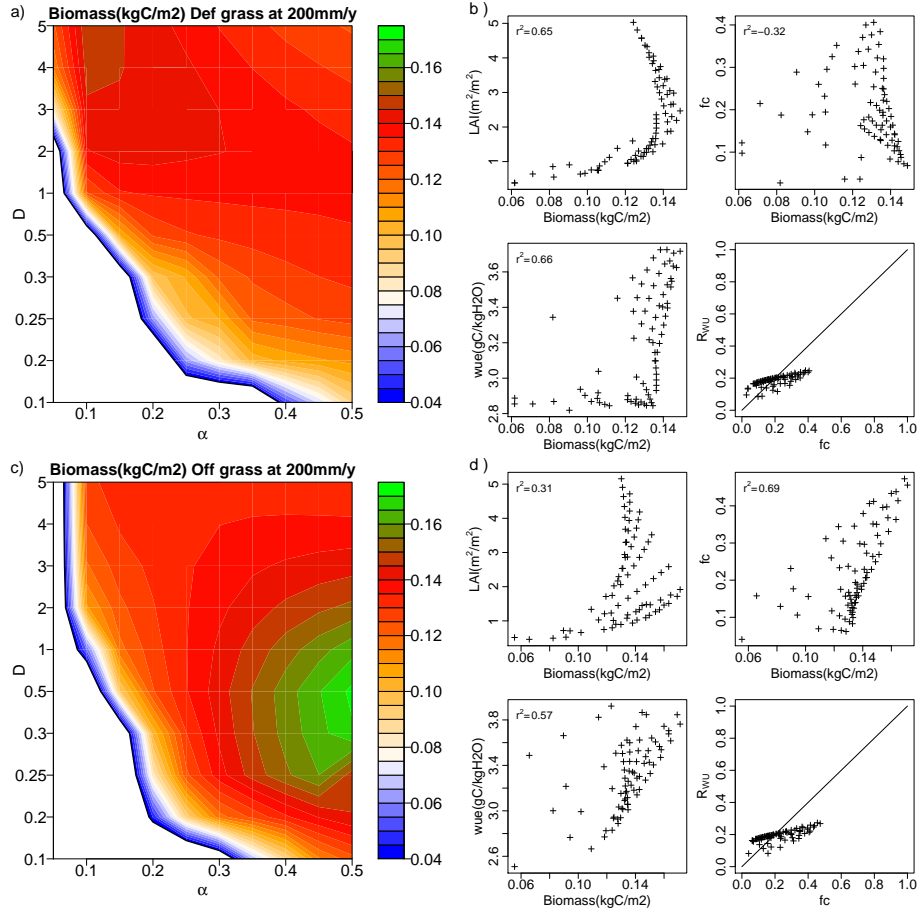


Figure 7: Sensitivity analysis of equilibrium biomass to vegetation structure: A. Panels (a) and (c) present six-year averaged total biomass that changes with different vegetation structures of two strategies. Patterns represent survival structures under the specified regime. Panels (b) and (d) display several variables (LAI, f_c and WUE) as a function of biomass and a comparison between f_c and R_{WU} . Solid lines in Panels (b) and (d) are one-one line. Panels (a) and (b) are for defensive grass case under 200 mm yr^{-1} . Panels (c) and (d) are for offensive grass case. The parameterization is based on C4 plants.

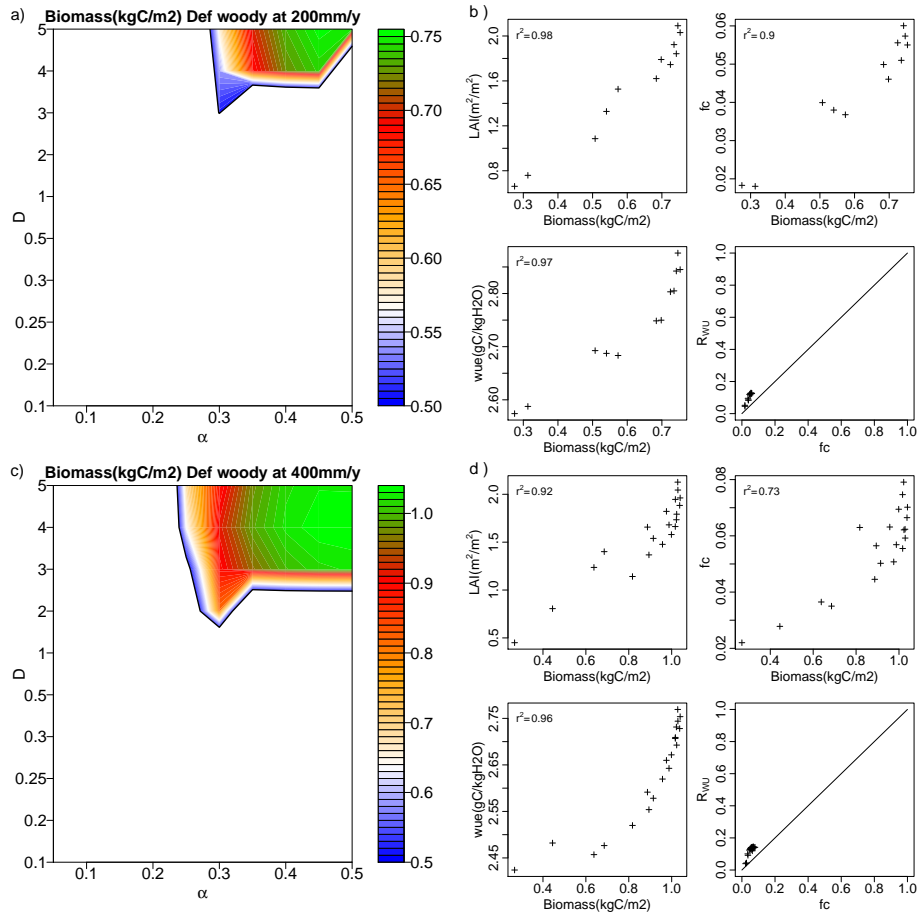


Figure 8: Sensitivity analysis of equilibrium biomass to vegetation structure: B. As Fig. 7, defensive woody vegetation case for 200 mm yr^{-1} (panels **a** and **b**) and 400 mm yr^{-1} (**c** and **d**).

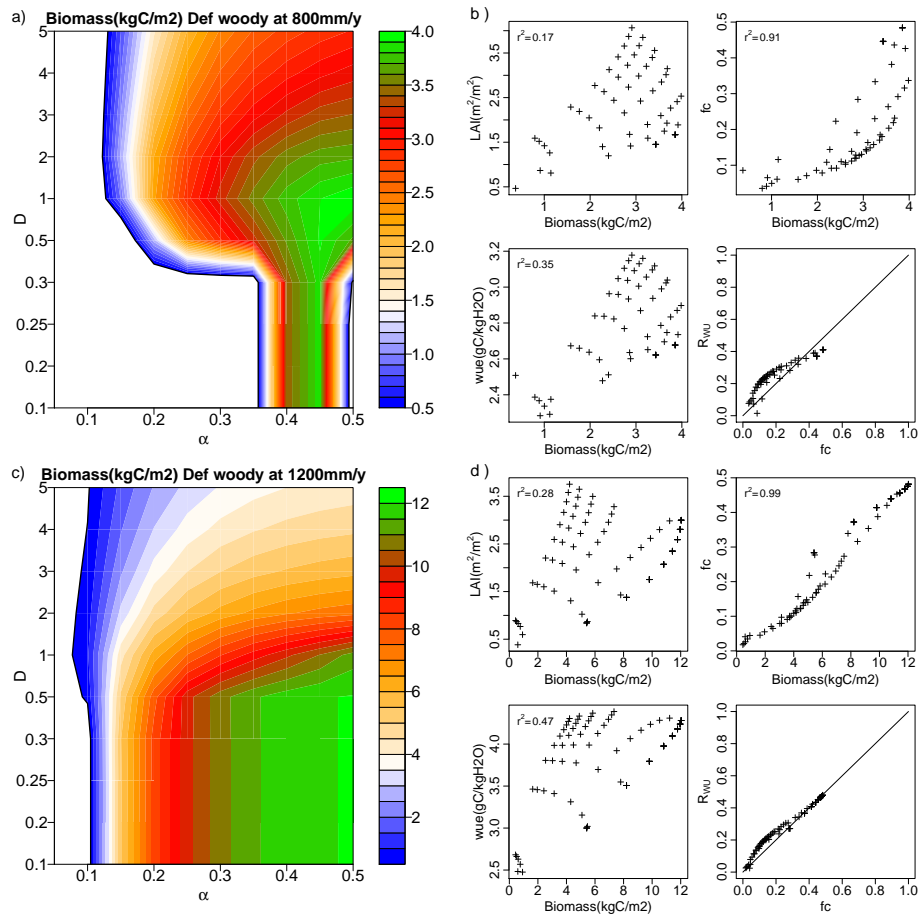


Figure 9: Sensitivity analysis of equilibrium biomass to vegetation structure: C. As Fig. 7 for 800 mm yr⁻¹ (panels a and b) and 1200 mm yr⁻¹ (c and d).

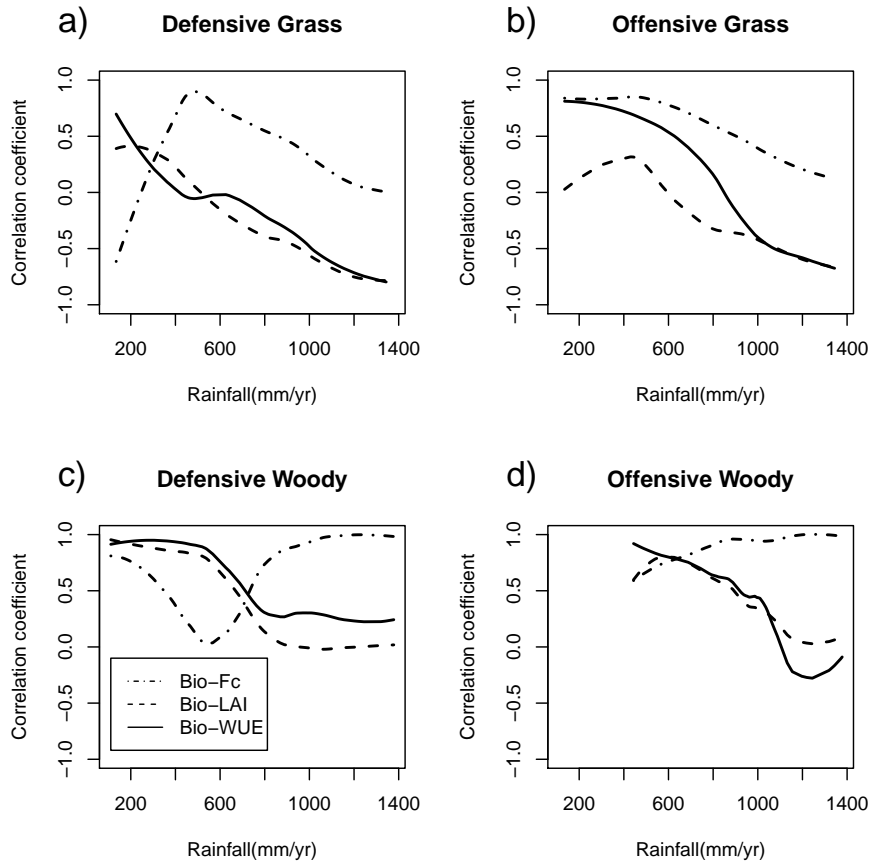


Figure 10: Dominant factor change with precipitation. Correlation coefficients between averaged biomass and three parameters as a function of mean annual precipitation. Panels (a), (b), (c) and (d) represent defensive grass, offensive grass, defensive woody and offensive woody respectively. Dot-dashed, dashed and solid lines are for correlation between biomass and f_c , LAI and WUE, respectively.